Vector and axial-vector mesons at finite temperature

S. Mallik[1], Sourav Sarkar[2]

[1] Saha Institute of Nuclear Physics, 1/AF, Bidhannagar, Kolkata-700064, India
[2] Variable Energy Cyclotron Centre, 1/AF, Bidhannagar, Kolkata-700064, India

Abstract. We consider the thermal correlation functions of vector and axial-vector currents and evaluate corrections to the vector and axial-vector meson pole terms to one loop in chiral perturbation theory. As expected, the pole positions do not shift to leading order in temperature. But the residues decrease with temperature. We review briefly other methods in the literature to determine these pole parameters. We find our evaluation to disprove a result on the mixing of the correlation functions at finite temperature.

1 Introduction

An important topic in the strong interaction at non-zero temperature is the calculation of shifts in the masses and the couplings which hadrons suffer while moving through a heat bath. Apart from their immediate relevance in understanding the experimental data on heavy ion collisions, these shifts as functions of temperature provide an effective description of the thermal properties of strong interaction. Mention must be made here also of the condensates, which are related more directly to the condensed matter aspects of the strong interaction, particularly to the possibility of a phase transition with the increase of temperature.

At low energies processes involving the strong interaction as described by QCD are best analysed in chiral perturbation theory [1]. It has long been established phenomenologically that the symmetry group $SU(3)_R \times SU(3)_L$ of the QCD Lagrangian of three flavours of massless quarks is broken spontaneously to its diagonal subgroup $SU(3)_V$, giving rise to the octet of Goldstone bosons. Chiral perturbation theory realises this symmetry non-linearly on the physical fields. This framework considerably restricts the interactions among hadrons involving the Goldstone bosons. It has led to a whole set of accurate analyses of low energy hadronic processes [2,3].

Chiral perturbation theory finds a natural application to problems of the strong interaction at non-zero temperature T. At low temperature pions dominate the heat bath, the other hadrons being exponentially suppressed. One is thus led to consider the reduced chiral symmetry group $G = SU(2)_R \times SU(2)_L$, which spontaneously breaks to the isospin subgroup $H = SU(2)_V$. This symmetry implies that interactions involving low energy pions are weak. In calculating quantities at low temperature these interactions can therefore be treated as a perturbation. A wide variety of problems has been treated in this way [4,5]. In

particular, it has been applied to the correlation function of nucleon currents to find the position of the nucleon pole and its residue at finite temperature [6]. In this work we apply a similar procedure to the isotriplets of vector and axial-vector mesons.

Here we consider the correlation functions of vector and axial-vector currents defined in QCD. To calculate the pole parameters to $O(T^2)$, we draw all the one loop Feynman diagrams with vector and axial-vector mesons and pions, which contribute to these correlation functions. With the form of interaction vertices prescribed by chiral perturbation theory, it is simple to evaluate the finite temperature parts of these diagrams near the poles in the chiral limit. Although we begin with a large number of diagrams, only a few actually contribute to the meson poles to order T^2. We also argue that other particles not included in our scheme cannot change the results to this order.

In Sect. 2 we summarise the chiral transformation rules of the relevant field variables to arrive at the chirally invariant Lagrangian of the spin-1 mesons and pions. In Sect. 3 we explicitly obtain the interaction vertices needed to evaluate the Feynman diagrams. In Sect. 4 we find the shift in the masses and couplings of these mesons to $O(T^2)$. Finally in Sect. 5 we summarise our results and comment on other attempts to determine these shifts. The appendix discusses the 2×2 matrix and the Lorentz tensor structures of the correlation functions in the real time thermal field theory.

2 Chiral perturbation theory

It is convenient to review in this section the definition of the appropriate field variables and their transformation properties, leading to the effective Lagrangian of chiral perturbation theory [7,8]. The Goldstone fields $\pi^a(x)$ re-

side in the coset space of G with respect to H. A standard parameterisation of this space allows one to collect these fields in the form of an unitary matrix,

$$u(x) = e^{i\pi(x)/2F_\pi}, \quad \pi(x) = \sum_{a=1}^{3} \pi^a(x)\tau^a, \qquad (2.1)$$

where the constant F_π can be identified with the pion decay constant, $F_\pi = 93\,\text{MeV}$, and τ^a are the Pauli matrices. The matrix u transforms under G according to the rule

$$u \to g_R u h^\dagger = h u g_L^\dagger, \qquad (2.2)$$

where $g_{R,L} \in SU(2)_{R,L}$ and $h(\pi) \in SU(2)_V$. The matrix $U = u^2$ then transforms as

$$U \to g_R U g_L^\dagger. \qquad (2.3)$$

Any multiplet $\psi(x)$ of non-Goldstone fields transforms as

$$\psi \to h\psi, \qquad (2.4)$$

with h in the appropriate representation. In particular, if they also belong to the adjoint (triplet) representation, such as the vector and the axial-vector mesons we are considering here, we may use the same h as in (2.2): Denoting the triplet fields by $R_\mu(x)$,

$$R_\mu(x) = \frac{1}{\sqrt{2}} \sum_{a=1}^{3} R_\mu^a(x)\tau^a, \qquad (2.5)$$

it transforms as

$$R_\mu \to h R_\mu h^\dagger. \qquad (2.6)$$

The singlet field $S_\mu(x)$, of course, remains unchanged, $S_\mu \to S_\mu$.

As already stated we are concerned here with the evaluation of the two-point functions of the vector and axial-vector currents of QCD,

$$V_\mu^a(x) = \bar{q}(x)\gamma_\mu \frac{\tau^a}{2} q(x), \quad A_\mu^a(x) = \bar{q}(x)\gamma_\mu \gamma_5 \frac{\tau^a}{2} q(x), \qquad (2.7)$$

in the effective field theory. This is most conveniently carried out in the external field method, where one introduces external fields $v_\mu^a(x)$ and $a_\mu^a(x)$ coupled to the currents $V_\mu^a(x)$ and $A_\mu^a(x)$ [1]. The original QCD Lagrangian $\mathcal{L}_{\text{QCD}}^{(0)}$ of massless quarks is then augmented to

$$\mathcal{L}_{\text{QCD}}^{(0)} + v_\mu^a(x)V_a^\mu(x) + a_\mu^a(x)A_a^\mu(x)$$
$$= i\bar{q}_R\gamma^\mu\{\partial_\mu - i(v_\mu + a_\mu)\}q_R$$
$$+ i\bar{q}_L\gamma^\mu\{\partial_\mu - i(v_\mu - a_\mu)\}q_L + \cdots \qquad (2.8)$$

where $q_R(q_L)$ is the right (left) handed component of q, $q_{R,L} = (1/2)(1 \pm \gamma_5)q$. The ellipsis denotes the (flavour neutral) gauge field term, and $v_\mu(x)$ and $a_\mu(x)$ are matrices in flavour space,

$$v_\mu(x) = \sum_{a=1}^{3} v_\mu^a(x)\frac{\tau^a}{2}, \quad a_\mu(x) = \sum_{a=1}^{3} a_\mu^a(x)\frac{\tau^a}{2}. \qquad (2.9)$$

The global invariance of $\mathcal{L}_{\text{QCD}}^{(0)}$ is now raised to local invariance under the transformations

$$q_R' = g_R q_R, \quad q_L' = g_L q_L,$$
$$v_\mu' \pm a_\mu' = g_{R,L}(v_\mu \pm a_\mu)g_{R,L}^\dagger + i g_{R,L}\partial_\mu g_{R,L}^\dagger, \quad (2.10)$$

where the group elements $g_{R,L}$ are now x-dependent.

The field strengths corresponding to the external potentials are given as usual by

$$F_{R,L}^{\mu\nu} = \partial^\mu(v^\nu \pm a^\nu) - \partial^\nu(v^\mu \pm a^\mu) - i[v^\mu \pm a^\mu, v^\nu \pm a^\nu]. \qquad (2.11)$$

The covariant derivatives of U and R_μ are given by

$$D_\mu U = \partial_\mu U - i(v_\mu + a_\mu)U + iU(v_\mu - a_\mu) \qquad (2.12)$$

and

$$\nabla_\mu R_\nu = \partial_\mu R_\nu + [\Gamma_\mu, R_\nu], \qquad (2.13)$$

with the connection

$$\Gamma_\mu = \frac{1}{2}\left(u^\dagger[\partial_\mu - i(v_\mu + a_\mu)]u + u[\partial_\mu - i(v_\mu - a_\mu)]u^\dagger\right). \qquad (2.14)$$

Thus the building elements of the effective Lagrangian are U, $D_\mu U$, $F_{R,L}^{\mu\nu}$, R_μ, S_μ and $\nabla_\mu R_\nu$.

Note that while some of the above variables (U, $D_\mu U$, $F_{R,L}^{\mu\nu}$) transform under the full group G, others (R_μ, S_μ and $\nabla_\mu R_\nu$) transform under the unbroken subgroup H. One may take advantage of the mixed transformation rule of u to redefine the former variables so as to transform under H only. Thus one introduces the field variables [7],

$$u_\mu = i u^\dagger D_\mu U u^\dagger = u_\mu^\dagger \qquad (2.15)$$

and

$$f_\pm^{\mu\nu} = \pm u^\dagger F_R^{\mu\nu}u + u F_L^{\mu\nu}u^\dagger. \qquad (2.16)$$

We now use these variables to write down the leading terms of the different pieces of the Lagrangian density, which are invariant under H and hence also under G. To calculate the correlation functions of isotriplets of vector and axial-vector currents, we need the Lagrangian for the interacting system of both the isotriplets and isosinglets of vector and axial-vector mesons and pions in the presence of the external fields. (We shall see later that other particles cannot contribute to the pole terms to order T^2.) For the pions we have the familiar term,

$$\mathcal{L}(\pi) = \frac{F_\pi^2}{4}\langle u_\mu u^\mu\rangle. \qquad (2.17)$$

Here and below the symbol $\langle A \rangle$ stands for the trace of the 2×2 matrix A. For the spin-1 meson isotriplet and isosinglet fields, let

$$R_{\mu\nu} = \nabla_\mu R_\nu - \nabla_\nu R_\mu, \quad S_{\mu\nu} = \partial_\mu S_\nu - \partial_\nu S_\mu. \qquad (2.18)$$

Then the kinetic terms take the form

$$\mathcal{L}_{\text{kin}}(R,S) = \sum\left(-\frac{1}{4}\langle R_{\mu\nu}R^{\mu\nu}\rangle + \frac{1}{2}m_R^2\langle R_\mu R^\mu\rangle\right)$$
$$+ \sum\left(-\frac{1}{4}S_{\mu\nu}S^{\mu\nu} + \frac{1}{2}m_S^2 S_\mu S^\mu\right), \quad (2.19)$$

where the two sums run over the isotriplets and the isosinglets respectively.

The leading coupling terms linear in the octets of the vector and the axial-vector fields have been obtained in [7,8] for the symmetry group $SU(3) \times SU(3)$. As mentioned already, the symmetry reduces to $SU(2) \times SU(2)$ at finite temperature. In effecting this reduction, we keep the masses of the physical particles in each of the octets the same but consider the interaction separately for the isotriplets $[\rho(770), a_1(1230)]$ and isosinglets $[\omega(782), f_1(1282)]$. Restricting to terms relevant to one loop calculations, we get for the vector meson couplings

$$\mathcal{L}_{\mathrm{int}}(V) = \frac{1}{2\sqrt{2}m_{\mathrm{V}}}(F_\rho \langle \rho_{\mu\nu} f_+^{\mu\nu} \rangle + \mathrm{i}G_\rho \langle \rho_{\mu\nu}[u^\mu, u^\nu] \rangle$$
$$+ \mathrm{i}H_\rho \langle \rho_\mu[u_\nu, f_-^{\mu\nu}] \rangle + H_\omega \epsilon_{\mu\nu\lambda\sigma} \omega^\mu \langle u^\nu f_+^{\lambda\sigma} \rangle), \quad (2.20)$$

while for the axial-vector meson such couplings are

$$\mathcal{L}_{\mathrm{int}}(A) = \frac{1}{2\sqrt{2}m_{\mathrm{A}}}(F_{a_1} \langle a_{1\mu\nu} f_-^{\mu\nu} \rangle \quad (2.21)$$
$$+ \mathrm{i}H_{a_1} \langle a_{1\mu}[u_\nu, f_+^{\mu\nu}] \rangle + H_{f_1} \epsilon_{\mu\nu\lambda\sigma} f_1^\mu \langle u^\nu f_-^{\lambda\sigma} \rangle).$$

Finally we write down the quadratic couplings of the triplets with the singlets and between themselves,

$$\mathcal{L}_{\mathrm{int}}(V, A) = \frac{1}{\sqrt{2}} \epsilon_{\mu\nu\lambda\sigma}(g_1 \omega^\mu \langle \rho^{\nu\lambda} u^\sigma \rangle + g_2 f_1^\mu \langle a_1^{\nu\lambda} u^\sigma \rangle)$$
$$+ \frac{\mathrm{i}}{2} g_3 \langle \rho^{\mu\nu}[a_{1\mu}, u_\nu] \rangle. \quad (2.22)$$

(The term $\langle a_1^{\mu\nu}[\rho_\mu, u_\nu] \rangle$ is equivalent to the third term above to leading order in pion momentum.) Although we have here a number of different coupling constants, only some of them will actually enter our results for the shifts in particle parameters to $O(T^2)$.

3 Perturbative vertices

The vertices needed in evaluating the one loop Feynman diagrams for the correlation functions can be recognised best from the diagrams themselves. Let us consider the correlation function of two vector currents at non-zero temperature $T = 1/\beta$,

$$\mathrm{i} \int \mathrm{d}^4x \mathrm{e}^{\mathrm{i}q \cdot x} \mathrm{Tr} \varrho T V_\mu^a(x) V_\nu^b(0), \quad (3.1)$$

where $\varrho = \mathrm{e}^{-\beta H}/\mathrm{Tr}\mathrm{e}^{-\beta H}$ is the thermal density matrix of QCD. The diagrams contributing to it are of three types, namely those of self-energy, vertex modification and intermediate states shown respectively in Figs. 1, 2 and 3. We see that we only need vertices up to four fields, counting both quantum (particle) and classical (external) fields. At each vertex the pion field can appear at most quadratically. When it does appear so, the two pion fields must be contracted at the same vertex. The resulting pion loop is of $O(T^2)$, if no derivative is present on the pion fields; but the loop is of higher order if it does, allowing us to ignore
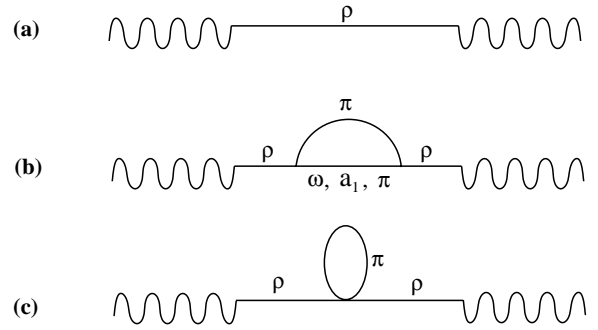

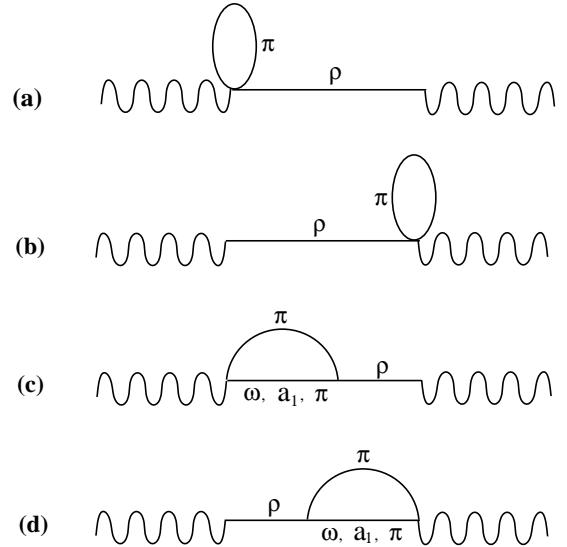Fig. 1a–c. ρ meson pole and self-energy diagrams

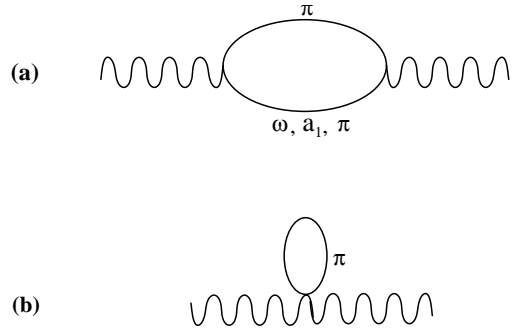
Fig. 2a–d. Vertex correction diagrams

Fig. 3a,b. Intermediate state diagrams

such vertices. Also at each vertex the external fields can occur at most linearly (with the exception of the vertex in Fig. 3b). At such a vertex with an external field, the vector or the axial-vector meson field must also occur linearly. Keeping these requirements in mind, we now obtain the polynomial version of the chiral Lagrangian written in the previous section.

The pion Lagrangian (2.17) can be expanded as

$$\mathcal{L}(\pi) = \frac{1}{2}(\partial_\mu \boldsymbol{\pi} \cdot \partial^\mu \boldsymbol{\pi} - m_\pi^2 \boldsymbol{\pi} \cdot \boldsymbol{\pi}) - F_\pi \boldsymbol{a}_\mu \cdot \partial^\mu \boldsymbol{\pi}$$
$$+ \boldsymbol{v}_\mu \cdot \boldsymbol{\pi} \times \partial^\mu \boldsymbol{\pi} + F_\pi \boldsymbol{\pi} \cdot (\boldsymbol{v}_\mu \times \boldsymbol{a}^\mu)$$
$$+ \frac{1}{2} F_\pi^2 \boldsymbol{a}_\mu \cdot \boldsymbol{a}^\mu + \frac{1}{2} \{ \boldsymbol{\pi} \cdot \boldsymbol{\pi}(\boldsymbol{v}_\mu \cdot \boldsymbol{v}^\mu - \boldsymbol{a}_\mu \cdot \boldsymbol{a}^\mu)$$
$$- \boldsymbol{v}_\mu \cdot \boldsymbol{\pi} \boldsymbol{v}^\mu \cdot \boldsymbol{\pi} + \boldsymbol{a}_\mu \cdot \boldsymbol{\pi} \boldsymbol{a}^\mu \cdot \boldsymbol{\pi} \} . \tag{3.2}$$

Here and below we denote the isovector triplet of fields by boldface letters. Note that we have added the pion mass term, even though we shall evaluate the final results in the chiral limit. The first term gives the free, thermal pion propagator matrix. As discussed in the appendix, all we need here is its 11-component,

$$\int \mathrm{d}^4 x \mathrm{e}^{\mathrm{i}k \cdot x} \mathrm{Tr} \varrho T \pi^a(x) \pi^b(0)|_{11} \tag{3.3}$$
$$= \delta^{ab} \left(\frac{\mathrm{i}}{k^2 - m_\pi^2 + \mathrm{i}\epsilon} + 2\pi n(k_0) \delta(k^2 - m_\pi^2) \right),$$

where n is the bosonic distribution function $n(k_0) = (\mathrm{e}^{\beta|k_0|} - 1)^{-1}$.

The kinetic part of the Lagrangian for the spin-1 mesons reduces to

$$\mathcal{L}_{\mathrm{kin}}(R, S)$$
$$= -\frac{1}{2} \sum_{\boldsymbol{\rho}, \boldsymbol{a}_1} \{ \partial_\mu \boldsymbol{R}_\nu \cdot (\partial^\mu \boldsymbol{R}^\nu - \partial^\nu \boldsymbol{R}^\mu) - m_R^2 \boldsymbol{R}_\mu \cdot \boldsymbol{R}^\mu \}$$
$$- \frac{1}{2} \sum_{\omega, f_1} \{ \partial_\mu S_\nu (\partial^\mu S^\nu - \partial^\nu S^\mu) - m_S^2 S_\mu S^\mu \}. \tag{3.4}$$

The densities of the spin-1 mesons are suppressed exponentially in the heat bath. So we need only the vacuum part of the respective 11-components of the propagator matrices, which for R_μ^a, for example, is

$$\int \mathrm{d}^4 x \mathrm{e}^{\mathrm{i}p \cdot x} \langle 0|T R_\mu^a(x) R_\nu^b(0)|0\rangle = \delta^{ab} \frac{\mathrm{i}(-g_{\mu\nu} + p_\mu p_\nu/m_R^2)}{p^2 - m_R^2 + \mathrm{i}\epsilon}. \tag{3.5}$$

As an illustration we now work out the vertices present in the term $\langle \rho_{\mu\nu} f_+^{\mu\nu} \rangle$. Since $f_+^{\mu\nu}$ is proportional to the external fields, we need only the terms in $\rho_{\mu\nu}$ without them. Thus up to four field vertices, we have

$$\langle \rho_{\mu\nu} f_+^{\mu\nu} \rangle = 4\langle \partial^\mu v^\nu (\partial_\mu \rho_\nu - \partial_\nu \rho_\mu) \rangle$$
$$+ \frac{2\mathrm{i}}{F_\pi} \langle \partial^\mu a^\nu [\pi, \partial_\mu \rho_\nu - \partial_\nu \rho_\mu] \rangle \tag{3.6}$$
$$- \frac{1}{2F_\pi^2} \langle \partial^\mu v^\nu [\pi, [\pi, \partial_\mu \rho_\nu - \partial_\nu \rho_\mu]] \rangle.$$

As already explained, we have to contract the two pion fields in the four field vertex above. Its thermal piece is

$$\mathrm{Tr} \varrho T \pi^a(x) \pi^b(x)|_{11} \rightarrow$$
$$\delta^{ab} \int \frac{\mathrm{d}^4 k}{(2\pi)^3} n(k_0) \delta(k^2 - m_\pi^2) = \delta^{ab} \frac{T^2}{12} \tag{3.7}$$

in the chiral limit. (We see here that any derivative on the pion fields would result in contributions of higher order in T). Thus the third term in (3.6) reduces to the first one with a T-dependent coefficient.

In this way we derive the pieces of the polynomial Lagrangian from those of the chiral Lagrangian of (2.20)–(2.22) as

$$\mathcal{L}(V) = \frac{F_\rho}{m_V} \left\{ \left(1 - \frac{T^2}{12F_\pi^2} \right) \partial^\mu \boldsymbol{v}^\nu \cdot (\partial_\mu \boldsymbol{\rho}_\nu - \partial_\nu \boldsymbol{\rho}_\mu) \right.$$
$$\left. + \frac{1}{F_\pi} \partial^\mu \boldsymbol{a}^\nu \cdot (\partial_\mu \boldsymbol{\rho}_\nu - \partial_\nu \boldsymbol{\rho}_\mu) \times \boldsymbol{\pi} \right\} \tag{3.8}$$
$$- \frac{2G_\rho}{m_V F_\pi^2} \partial_\mu \boldsymbol{\rho}_\nu \cdot \partial^\mu \boldsymbol{\pi} \times \partial^\nu \boldsymbol{\pi} - \frac{\sqrt{2} H_\omega}{m_V F_\pi} \epsilon_{\mu\nu\lambda\sigma} \omega^\mu \partial^\nu \boldsymbol{\pi} \cdot \partial^\lambda \boldsymbol{v}^\sigma,$$

$$\mathcal{L}(A) = -\frac{F_{a_1}}{m_A} \left\{ \left(1 - \frac{T^2}{12F_\pi^2} \right) \partial^\mu \boldsymbol{a}^\nu \cdot (\partial_\mu \boldsymbol{a}_{1\nu} - \partial_\nu \boldsymbol{a}_{1\mu}) \right.$$
$$\left. + \frac{1}{F_\pi} \partial^\mu \boldsymbol{v}^\nu \cdot (\partial_\mu \boldsymbol{a}_{1\nu} - \partial_\nu \boldsymbol{a}_{1\mu}) \times \boldsymbol{\pi} \right\}$$
$$+ \frac{\sqrt{2} H_{f_1}}{m_A F_\pi} \epsilon_{\mu\nu\lambda\sigma} f_1^\mu \partial^\nu \boldsymbol{\pi} \cdot \partial^\lambda \boldsymbol{a}^\sigma, \tag{3.9}$$

and $[u \overset{\leftrightarrow}{\partial_\mu} v \equiv (\partial_\mu u)v - u\partial_\mu v]$ as

$$\mathcal{L}(V, A)$$
$$= \epsilon_{\mu\nu\lambda\sigma} \left(\frac{g_1}{F_\pi} \omega^\mu \overset{\leftrightarrow}{\partial^\nu} \boldsymbol{\rho}^\lambda \cdot \partial^\sigma \boldsymbol{\pi} + \frac{g_2}{F_\pi} f_1^\mu \overset{\leftrightarrow}{\partial^\nu} \boldsymbol{a}_1^\lambda \cdot \partial^\sigma \boldsymbol{\pi} \right)$$
$$+ \frac{g_3}{F_\pi} \partial^\mu \boldsymbol{\rho}^\nu \cdot (\boldsymbol{a}_{1\mu} \times \partial_\nu \boldsymbol{\pi} - \boldsymbol{a}_{1\nu} \times \partial_\mu \boldsymbol{\pi}). \tag{3.10}$$

In writing the above expressions, when two or more vertices present themselves with the same field content, differing only in the number of derivatives on the pion field, we retain only the one with fewer or no derivatives on it.

The coupling constants can generally be determined from the observed decay rates of the particles. Thus the decay rate $\Gamma(\rho^0 \rightarrow e^+ e^-) = 6.9\,\mathrm{keV}$ gives $F_\rho = 154\,\mathrm{MeV}$. Similarly the decay rate $\Gamma(a_1 \rightarrow \pi\gamma) = 640\,\mathrm{keV}$ gives $F_{a_1} = 135\,\mathrm{MeV}$. The latter constant can also be determined from one of the Weinberg sum rules [9], agreeing closely with this value. The decay width $\Gamma(\rho \rightarrow 2\pi) = 153\,\mathrm{MeV}$ gives the coupling $G_\rho = 69\,\mathrm{MeV}$. Here one expects large chiral corrections as the pions are far from being soft. Thus the chiral loops reduce this value to $G_\rho = 53\,\mathrm{MeV}$ [7]. Using this value and the decay rate $\Gamma(\omega \rightarrow 3\pi) = 7.6\,\mathrm{MeV}$, we get the dimensionless coupling constant $g_1 = 0.87$ [10]. There do not appear any data relating to the decay of f_1 to determine g_2. The remaining coupling constants in (3.8)–(3.10) will not appear in our results to $O(T^2)$.

4 Mass and coupling shifts

Given the vertices, it is simple to calculate the diagrams of Figs. 1–3. The Lorentz tensor and the thermal matrix structures of the two-point functions are discussed in the

appendix, according to which the free pole term of Fig. 1a is given in the variable $E \equiv q_0$ for $\boldsymbol{q} = 0$ essentially by

$$-E^4 \cdot \frac{(F_\rho/m_V)^2}{E^2 - m_V^2 + i\epsilon}.$$

We now determine how this pole position and the residue are modified by interactions at finite temperature. The self-energy diagrams of Fig. 1 modify it to

$$-E^4 \cdot (F_\rho/m_V)^2/(E^2 - m_V^2 - \Pi_t),$$

where we use (A.12) and (A.13) to construct Π_t from the finite temperature part of the polarisation tensor $\Pi_{\alpha\beta}$,

$$\Pi_{\alpha\beta}(q) = \sum_{c=\omega, a_1, \pi} \Pi_{\alpha\beta}^{(c)}(q), \tag{4.1}$$

the sum running over the diagrams of Fig. 1b. (We have left out Fig. 1c, which is clearly of order T^4.) To write out these contributions we define the gauge invariant tensors

$$A_{\alpha\beta}(q) = -g_{\alpha\beta} + q_\alpha q_\beta/q^2,$$
$$B_{\alpha\beta}(q, k) = q^2 k_\alpha k_\beta - q \cdot k(q_\alpha k_\beta + k_\alpha q_\beta) + (q \cdot k)^2 g_{\alpha\beta},$$
$$C_{\alpha\beta}(q, k) = q^4 k_\alpha k_\beta - q^2(q \cdot k)(q_\alpha k_\beta + k_\alpha q_\beta)$$
$$+ (q \cdot k)^2 q_\alpha q_\beta. \tag{4.2}$$

The three contributions are now given by

$$\Pi_{\alpha\beta}^{(\omega)} = -\left(\frac{2g_1}{F_\pi}\right)^2 \tag{4.3}$$
$$\times \int \frac{\mathrm{d}^4 k}{(2\pi)^3} \frac{n(k_0)\delta(k^2 - m_\pi^2)}{(q-k)^2 - m_V^2}(q^2 k^2 A_{\alpha\beta} + B_{\alpha\beta}),$$

$$\Pi_{\alpha\beta}^{(a_1)} = -2\left(\frac{g_3}{F_\pi}\right)^2 \tag{4.4}$$
$$\times \int \frac{\mathrm{d}^4 k}{(2\pi)^3} \frac{n(k_0)\delta(k^2 - m_\pi^2)}{(q-k)^2 - m_A^2}(B_{\alpha\beta} - C_{\alpha\beta}/m_A^2)$$

and

$$\Pi_{\alpha\beta}^{(\pi)} = 2\left(\frac{2G_\rho}{m_V F_\pi^2}\right)^2 \int \frac{\mathrm{d}^4 k}{(2\pi)^3} \frac{n(k_0)\delta(k^2 - m_\pi^2)}{(q-k)^2 - m_\pi^2} C_{\alpha\beta}. \tag{4.5}$$

The respective contributions to Π_t are ($\omega_k = (\boldsymbol{k}^2 + m_\pi^2)^{1/2}$)

$$\Pi_t^{(\omega)}(E) = \frac{16g_1^2}{3F_\pi^2} E^2(E^2 - m_V^2 + m_\pi^2) \tag{4.6}$$
$$\times \int \frac{\mathrm{d}^3 k \, n(\omega_k)}{(2\pi)^3 2\omega_k} \cdot \frac{\boldsymbol{k}^2}{(E^2 - m_V^2 + m_\pi^2)^2 - 4E^2\omega_k^2},$$

$$\Pi_t^{(a_1)}(E) = \frac{4}{3}\left(\frac{g_3}{F_\pi}\right)^2 E^2(E^2 - m_A^2 + m_\pi^2) \tag{4.7}$$
$$\times \int \frac{\mathrm{d}^3 k \, n(\omega_k)}{(2\pi)^3 2\omega_k} \cdot \frac{\boldsymbol{k}^2(2 + E^2/m_A^2) + 3m_\pi^2}{(E^2 - m_A^2 + m_\pi^2)^2 - 4E^2\omega_k^2}$$

and

$$\Pi_t^{(\pi)}(E) = \frac{4}{3}\left(\frac{2G_\rho}{m_V F_\pi^2}\right)^2 E^6 \int \frac{\mathrm{d}^3 k \, n(\omega_k)}{(2\pi)^3 2\omega_k} \cdot \frac{\boldsymbol{k}^2}{E^4 - 4E^2\omega_k^2}. \tag{4.8}$$

To evaluate the integrals for E^2 near m_V^2 in the chiral limit, we note the difference in the small $\boldsymbol{k}$ behaviour of the denominators of the integrands: while it behaves like $\sim \boldsymbol{k}^2$ in (4.6), they are constants in (4.7) and (4.8). Accordingly we get [11]

$$\Pi_t^{(\omega)}(E) = -\frac{g_1^2 T^2}{18F_\pi^2}(E^2 - m_V^2), \quad \Pi_t^{(a_1)} \sim \Pi_t^{(\pi)} \sim O(T^4). \tag{4.9}$$

A comment on this evaluation is in order. One might think that the equality of the masses of ρ and ω is necessary to arrive at the T^2 behaviour of the integral in (4.6), which would otherwise behave as T^4. But this is actually not the case from the point of view of the physics at hand. Let us take physical masses for the two mesons with a mass difference $\sim 10\,\mathrm{MeV}$. Then for temperatures small compared to $10\,\mathrm{MeV}$, the leading behaviour of the integral is indeed $\sim T^4$. However, as the temperature increases, this behaviour goes over to one of T^2. Since we are really interested in temperatures much higher than several MeVs, it is the T^2 behaviour which is of relevance here.

Taking into account the self-energy correction given by (4.9) and the constant vertex corrections from Fig. 2a,b, we get for the complete pole term

$$-E^4 \frac{(F_\rho^T/m_V)^2}{E^2 - m_V^2}, \tag{4.10}$$

with

$$F_\rho^T = F_\rho \left\{1 - \left(1 + \frac{g_1^2}{3}\right)\frac{T^2}{12F_\pi^2}\right\}. \tag{4.11}$$

It is simple to see that the remaining diagrams cannot alter this pole term to $O(T^2)$. Each of the remaining vertex corrections of Fig. 2c,d is essentially of the form of the corresponding self-energy integral (Π_t) multiplied by the ρ-meson pole. Then the behaviour (4.9) of the self-energies excludes any pole contribution to $O(T^2)$ from these corrections. Of the contributions from the diagrams of Fig. 3 with intermediate states, the one with $\pi\omega$ is like $\Pi_t^{(\omega)}$, while those with πa_1 and $\pi\pi$ have two powers of $\boldsymbol{k}$ fewer in the integrands compared to the self-energies $\Pi_t^{(a_1)}$ and $\Pi_t^{(\pi)}$ respectively. Clearly these cannot contribute to the ρ-meson pole.

It is now also simple to establish that any particle with a mass other than m_V and not included in our calculation cannot alter our results. The argument rests simply on the structure of the interaction vertices without external fields. Such a vertex must have a pion field with a derivative. Thus the loop integrals involving such a particle must be of order higher than T^2.

It is interesting to work out the amplitude of Fig. 3a corresponding to the intermediate state πa_1. Its finite temperature part is given by

$$-2\left(\frac{F_{a_1}}{m_A F_\pi}\right)^2 \int \frac{\mathrm{d}^4 k}{(2\pi)^3} \frac{n(k_0)\delta(k^2 - m_\pi^2)}{(q-k)^2 - m_A^2}$$
$$\times \{q^2(q^2 - 2q \cdot k)A_{\mu\nu} - B_{\mu\nu}\}. \tag{4.12}$$

It may be readily evaluated in the chiral limit to give essentially [11]

$$\frac{T^2}{6F_\pi^2}\left\{-E^4\frac{(F_{a_1}/m_\mathrm{A})^2}{E^2-m_\mathrm{A}^2}\right\},\qquad(4.13)$$

where the expression in second bracket is the contribution of the axial-vector meson a_1 to the vacuum correlation function of the axial-vector currents. Observe the different origin of the $O(T^2)$ correction to the ρ and a_1 poles. While for ρ it is given by the self-energy due to the $\pi\omega$ and constant vertex diagram, it is given by the intermediate state πa_1 for a_1. This presence of an *axial*-vector meson pole in the *vector* current correlation function at finite temperature was detected earlier using PCAC and current algebra [12].

One can calculate the axial-vector meson pole term in the axial-vector current correlation function in an entirely analogous manner. Again one finds that the pole position does not shift from $E^2 = m_\mathrm{A}^2$, and the residue $F_{a_1}^T$ is given by (4.11) with g_1 replaced by g_2.

5 Discussion

Here we have determined the temperature dependence of the parameters of the ρ- and a_1-meson poles appearing in the vector and the axial-vector correlation functions. It is based on the flavour symmetry of QCD and its spontaneous breakdown, as embodied in chiral perturbation theory. It allows for a low temperature expansion of these quantities, of which we just calculate the leading term to $O(T^2)$. To this order the mass shift is zero, due to the presence of derivatives on the pion fields in interaction vertices as required by the chiral symmetry. The residues depend on the coupling constants at the vertices $\rho\omega\pi$ and $a_1 f_1 \pi$ and decrease with temperature. These results parallel those for the nucleon calculated earlier, the above vertices playing roles analogous to that of the vertex $\pi N\bar{N}$ [6].

We may try to estimate the range of validity of our results by comparing these with the temperature expansions of other quantities. For the quark condensate the expansion has been worked out to order T^6 [4]. It shows that the T^2 term continues to dominate the series up to $T = 150\,\mathrm{MeV}$. This may not be true in all cases, however. Take the example of the nucleon pole residue in the nucleon correlation function. In the pion–nucleon system there is the low energy resonance $\Delta(1237)$, which limits considerably the range of validity of the first few terms in the chiral perturbation series for πN scattering amplitudes. Already at $T = 100\,\mathrm{MeV}$, the average pion energies in the heat bath are outside this range. This situation limits the validity of the T^2 term in the nucleon pole residue to temperatures below $100\,\mathrm{MeV}$.

As the $\pi\rho$ and πa_1 systems do not have any such low energy excitations, we may expect our calculation to order T^2 to represent the expansion well up to temperatures of about $150\,\mathrm{MeV}$, as in the case of the quark condensate.

There is, however, one source of enhanced chiral corrections to our results, which may limit this range of validity. As mentioned earlier, at the vertices where the ρ or the external fields couple to two pions (see Figs. 1b, 2c,d and 3a), the pion momenta are not at all soft. Thus, although these diagrams do not contribute to order T^2, the coefficients of higher order terms may be larger.

We finally comment briefly on the different approaches in the literature to determine the temperature dependence of these parameters. First, there are other Lagrangian approaches. One has the massive Yang–Mills [13] and the hidden gauge [14] formulations. Since these Lagrangians are built on the $SU(2)\times SU(2)$ flavour symmetry, they also produce no shift in the meson masses to $O(T^2)$ [15,16]. However, the coefficients of T^4 quoted in these works must be incomplete, as they do not include two loop diagrams. One has also the more phenomenological Lagrangian of quantum hadrodynamics [17], which produces a negligible shift in the meson masses to $O(T^2)$ [18].

The second approach tries to calculate the correlation functions using soft pion techniques, but fails to reproduce the terms proportional to g_1^2 and g_2^2 in F_ρ and F_{a_1}, respectively [12]. Since chiral perturbation theory actually incorporates such techniques in a systematic and refined way, it is interesting to trace this disagreement. The Tr(ace) in (3.1) can be restricted to the vacuum and the one pion states, giving the full contribution to $O(T^2)$ in the chiral limit. In the pion matrix element one may use the hypotheses of the partially conserved axial-vector current and the algebra of currents to arrive at

$$\mathrm{Tr}\varrho TV_\mu^a(x)V_\nu^b(0)=\left(1-\frac{T^2}{6F_\pi^2}\right)\langle0|TV_\mu^a(x)V_\nu^b(0)|0\rangle_\beta$$
$$+\frac{T^2}{6F_\pi^2}\langle0|TA_\mu^a(x)A_\nu^b(0)|0\rangle,$$

and a similar one for the axial-vector correlation function. The subscript β in the first matrix element on the right is a reminder that it is really not a vacuum matrix element, since any internal (pion) line which would occur in its perturbative evaluation must be taken as thermal. Being multiplied with T^2, the second matrix element can be taken as a true vacuum expectation value for results to $O(T^2)$ and we have already verified the correctness of this term in our calculations above.

The authors of [12] assume the first matrix element also to be a true vacuum matrix element having no temperature dependence. In terms of Feynman diagrams it amounts to ignoring the temperature dependence of the self-energy diagrams of Fig. 1, which can in general contribute to both the pole position and the residue. In fact, the missing g_1^2 term in F_ρ arises exactly from the self-energy diagram of Fig. 1b. A similar situation arises in the case of the correlation function of nucleon currents. Applying the same soft pion techniques and assuming the resulting matrix elements to be true vacuum expectation values [19], one misses the term proportional to the axial coupling constant of the nucleon in the residue of the nucleon pole [6]. We conclude that such soft pion techniques

as applied to the thermal correlation functions cannot reproduce the full results of chiral perturbation theory.

The third approach is based on thermal QCD sum rules [20,21]. It is convenient to discuss these sum rules after subtracting the corresponding vacuum sum rules, leaving only T-dependent contributions. The spectral side of such a sum rule is given by three types of one loop diagrams, like those of Figs. 1, 2 and 3. In the literature, however, it is assumed to be saturated by a pole term with T-dependent parameters and the two particle intermediate states containing (at least) one pion. The inadequacy of this saturation scheme is revealed by the fact that the self-energy and vertex correction diagrams are generally not exhausted by contributions which make the pole term T-dependent. It is the neglect of the remaining contributions which make the existing results unreliable. (For the incorporation of such remaining contributions in the nucleon sum rule, see [19,22].)

The fourth and the last one is a phenomenological approach based on the (first order) virial expansion of the self-energy of a particle [6,23]. Quite generally it expresses the complex shift in the pole position of a particle as an integral over the product of the forward scattering amplitude of a pion on the particle and the pion distribution function. Since the pion gas is rather dilute even at a temperature $\sim 100\,\text{MeV}$, this formula should hold up to higher temperatures than the results of a chiral perturbation expansion to first order only. But the problem here is to construct the scattering amplitude, which is reliable [24].

Appendix

Here we discuss the kinematic structure of the vector and axial-vector two-point functions. In the real time formulation of thermal field theory we are using here, one has with each physical vertex an associated (ghost) vertex to take into account [25]. This causes all two-point functions to take the form of 2×2 matrices. Thus even if we begin with the 11-component, the perturbative expansion will mix it up with the other components. But as we show below, this complication does not arise for the problem at hand and we actually need work with the 11-component only.

Consider first the complete vector (or axial-vector) meson propagator, which appears in the self-energy diagrams of Fig. 1. Denoting the thermal 2×2 matrices in this appendix by boldface letters, it satisfies the Dyson equation,

$$\boldsymbol{D}_{\mu\nu} = \boldsymbol{D}_{\mu\nu}^{(0)} + \boldsymbol{D}_{\mu\lambda}^{(0)}(-\mathrm{i}\boldsymbol{\Pi}^{\lambda\sigma})\boldsymbol{D}_{\sigma\nu}. \qquad (A.1)$$

The free thermal propagator has the factorised form

$$\boldsymbol{D}_{\mu\nu}^{(0)}(q_0, \boldsymbol{q}) = \boldsymbol{U}(q_0)\begin{pmatrix} D_{\mu\nu}^{(0)} & 0 \\ 0 & D_{\mu\nu}^{(0)*} \end{pmatrix}\boldsymbol{U}(q_0), \qquad (A.2)$$

where

$$\boldsymbol{U}(q_0) = \begin{pmatrix} \sqrt{1+n} & \sqrt{n} \\ \sqrt{n} & \sqrt{1+n} \end{pmatrix}, \quad n = (\mathrm{e}^{\beta|q_0|}-1)^{-1}, \ (A.3)$$

and $D_{\mu\nu}^{(0)}(q)$ is the vacuum propagator

$$D_{\mu\nu}^{(0)}(q) = \frac{\mathrm{i}(-g_{\mu\nu} + q_\mu q_\nu/m_{\mathrm{R}}^2)}{q^2 - m_{\mathrm{R}}^2 + \mathrm{i}\epsilon}. \qquad (A.4)$$

From its spectral representation, the complete propagator $\mathrm{i}\boldsymbol{D}_{\mu\nu}(q)$ can also be shown to admit a similar factorisation [26]:

$$\boldsymbol{D}_{\mu\nu}(q_0, \boldsymbol{q}) = \boldsymbol{U}(q_0)\begin{pmatrix} D_{\mu\nu} & 0 \\ 0 & D_{\mu\nu}^{*} \end{pmatrix}\boldsymbol{U}(q_0). \qquad (A.5)$$

It then follows from (A.1) that $\boldsymbol{U}(-\mathrm{i}\boldsymbol{\Pi}_{\mu\nu})\boldsymbol{U}$ must have the diagonal structure:

$$\boldsymbol{U}(-\mathrm{i}\boldsymbol{\Pi}_{\mu\nu})\boldsymbol{U} = \begin{pmatrix} -\mathrm{i}\Pi_{\mu\nu} & 0 \\ 0 & \mathrm{i}\Pi_{\mu\nu}^* \end{pmatrix} \qquad (A.6)$$

The matrix equation (A.1) now collapses to the ordinary equation

$$D_{\mu\nu} = D_{\mu\nu}^{(0)} + D_{\mu\lambda}^{(0)}(-\mathrm{i}\Pi^{\lambda\sigma})D_{\sigma\nu} \qquad (A.7)$$

and its complex conjugate. The only remnants of the matrix structure are the relations between $\Pi_{\mu\nu}$ and the components of $\boldsymbol{\Pi}_{\mu\nu}$. With the 11-component of the latter, these are

$$\mathrm{Re}(\boldsymbol{\Pi}_{11})_{\mu\nu} = \mathrm{Re}\Pi_{\mu\nu}, \quad \mathrm{Im}(\boldsymbol{\Pi}_{11})_{\mu\nu} = (1+2n)\mathrm{Im}\Pi_{\mu\nu}. \qquad (A.8)$$

In calculations at finite temperature, one usually prefers the matter rest frame, thereby losing explicit Lorentz covariance. The latter may be restored by bringing in the four velocity u_μ in the medium[1]. Then the time and space components of a four-vector q_μ are converted to Lorentz scalars, $\omega = u \cdot q$ and $\bar{q} = (\omega^2 - q^2)^{1/2}$. In this framework a gauge covariant decomposition of the polarisation tensor is

$$\Pi_{\mu\nu}(q) = \Pi_t P_{\mu\nu} + \Pi_l Q_{\mu\nu}, \qquad (A.9)$$

where we choose the kinematic covariants as

$$P_{\mu\nu} = -g_{\mu\nu} + \frac{q_\mu q_\nu}{q^2} - \frac{q^2}{\bar{q}^2}\tilde{u}_\mu\tilde{u}_\nu, \quad Q_{\mu\nu} = \frac{q^4}{\bar{q}^2}\tilde{u}_\mu\tilde{u}_\nu, \ (A.10)$$

with $\tilde{u}_\mu = u_\mu - \omega q_\mu/q^2$. The invariant amplitudes are functions of two variables, say q^2 and ω. With the decomposition (A.9) the Dyson equation (A.7) can be solved to get

---

[1] No confusion should arise from the earlier use of u_μ as a field variable in Sect. 2

$$D_{\mu\nu} = \frac{\mathrm{i}}{q^2 - m_{\mathrm{R}}^2 - \Pi_t + \mathrm{i}\epsilon} P_{\mu\nu}$$
$$+ \frac{\mathrm{i}}{q^2 - m_{\mathrm{R}}^2 - q^2 \Pi_l + \mathrm{i}\epsilon} \frac{Q_{\mu\nu}}{q^2} + \frac{\mathrm{i}}{m_{\mathrm{R}}^2} \frac{q_\mu q_\nu}{q^2} .\text{(A.11)}$$

To find the invariant amplitudes $\Pi_{t,l}$ we form the scalars

$$\Pi_1 = \Pi_\mu^\mu, \quad \Pi_2 = u^\mu u^\nu \Pi_{\mu\nu}, \qquad \text{(A.12)}$$

while (A.9) gives

$$\Pi_l = \frac{1}{\bar{q}^2} \Pi_2, \quad \Pi_t = -\frac{1}{2}\left(\Pi_1 + \frac{q^2}{\bar{q}^2}\Pi_2\right). \qquad \text{(A.13)}$$

In the limit $\boldsymbol{q} \to 0$, the kinematic structures (A.10) relate the two invariant amplitudes,

$$\Pi_t(q_0, \boldsymbol{q}=0) = q_0^2 \Pi_l(q_0, \boldsymbol{q}=0). \qquad \text{(A.14)}$$

In this limit the second equation of (A.13) simplifies to

$$\Pi_t = -\frac{1}{3}\Pi_1. \qquad \text{(A.15)}$$

Having discussed the 2×2 matrix structure of the complete propagator, we turn to the same for the two-point functions, where for definiteness we take the one for the vector currents. From the self-energy diagrams of Fig. 1 this gets the contribution

$$\delta^{ab}\left(\frac{F_{\mathrm{V}}}{m_{\mathrm{V}}}\right)^2 (q^2 g_\mu^\lambda - q_\mu q^\lambda) \boldsymbol{D}_{\lambda\sigma}(q^2 g_\nu^\sigma - q^\sigma q_\nu)$$

$$= \delta^{ab}\boldsymbol{U}(q_0)\begin{pmatrix} G_{\mu\nu} & 0 \\ 0 & -G_{\mu\nu}^* \end{pmatrix}\boldsymbol{U}(q_0), \qquad \text{(A.16)}$$

where

$$G_{\mu\nu} = -q^4\left(\frac{F_\rho}{m_{\mathrm{V}}}\right)^2 \qquad\qquad\qquad \text{(A.17)}$$

$$\times \left(\frac{1}{q^2 - m_{\mathrm{V}}^2 - \Pi_t + \mathrm{i}\epsilon}P_{\mu\nu} + \frac{1}{q^2 - m_{\mathrm{V}}^2 - q^2\Pi_l + \mathrm{i}\epsilon}\frac{Q_{\mu\nu}}{q^2}\right)$$

on using (A.11). Note that at $\boldsymbol{q} = 0$ the two pole positions above coincide due to the kinematic constraint (A.14). The vertex correction diagrams of Fig. 2c,d are of the form

$$\boldsymbol{\Pi}^{\mu\lambda}\boldsymbol{D}_{\lambda\nu}^{(0)} = \boldsymbol{U}^{-1}(q_0)\begin{pmatrix} \Pi^{\mu\lambda}D_{\lambda\nu}^{(0)} & 0 \\ 0 & \Pi^{\mu\lambda*}D_{\lambda\nu}^{(0)*} \end{pmatrix}\boldsymbol{U}(q_0),$$
$$\text{(A.18)}$$

while the diagrams Fig. 3a with intermediate states are of the form given by (A.5).

We see that the results of the evaluation of different diagrams are typically of the form of a diagonal matrix, sandwiched between $\boldsymbol{U}$ or $\boldsymbol{U}^{-1}$. Near the meson pole the $\boldsymbol{U}$ matrix reduces to the unit matrix with exponential cor-

rection $\sim \mathrm{e}^{-m_\rho/T}$. Such corrections are too small to be retained when we are calculating corrections of $O(T^2)$ only. The remaining diagonal matrix may be represented by its 11-component, which again admits a decomposition into invariant amplitudes like that of $\Pi_{\mu\nu}$ in (A.9) with the longitudinal and the transverse ones being again related for $\boldsymbol{q} = 0$ as in (A.14) for $\Pi_{l,t}$.

References

1. J. Gasser, H. Leutwyler, Ann. Phys. 142 (1984); Nucl. Phys. B **250**, 465 (1985)
2. J. Gasser, H. Leutwyler, Nucl. Phys. B **250**, **517**, 539 (1985)
3. For a review see G. Ecker, Prog. Part. and Nuc. Phys. **35**, 1 (1995)
4. J. Gasser, H. Leutwyler, Phys. Lett. B **184**, 83 (1987); P. Gerber, H. Leutwyler, Nucl. Phys. B **231**, 387 (1989)
5. J. Gasser, H. Leutwyler, Phys. Lett. B **188**, 477 (1987); J. Goity, H. Leutwyler, Phys. Lett. B **228**, 517 (1989)
6. H. Leutwyler, A.V. Smilga, Nucl. Phys. B **342**, 302 (1990)
7. G. Ecker, J. Gasser, A. Pich, E. de Rafael, Nucl. Phys. B **321**, 311 (1989)
8. G. Ecker, J. Gasser, H. Leutwyler, A. Pich, E. de Rafael, Phys. Lett. B **223**, 425 (1989)
9. S. Weinberg, Phys. Rev. Lett. **18**, 507 (1967)
10. M. Gell-Mann, D. Sharp, W.G. Wagner, Phys. Rev. Lett. **8**, 261 (1962)
11. A more satisfactory way to calculate these results is to obtain first the absorptive parts of the loop integrals and then reconstruct the amplitudes using dispersion relations
12. M. Dey, V.L. Eletsky, B.L. Ioffe, Phys. Lett B **252**, 620 (1990);
    V.L. Eletsky, B.L. Ioffe, Phys. Rev. D **47**, 3083 (1993)
13. U.-G. Meissner, Phys. Rep. **161**, 213 (1988)
14. M. Bando, T. Kugo, K. Yamawaki, Phys. Rep. **164**, 217 (1988)
15. M. Harada, A. Shibata, Phys. Rev. D **55**, 6716 (1997)
16. C. Song, Phys. Rev D **48**, 1375 (1993); D **53**, 3962 (1996)
17. B.D. Serot, J.D. Walecka, Advances in Nuclear Physics, vol. 16;
    S.A. Chin, Ann. Phys. **108**, 301 (1977)
18. J. Alam, S. Sarkar, P. Roy, T. Hatsuda, B. Sinha, Ann. Phys. (N.Y.) **286**, 159 (2000)
19. Y. Koike, Phys. Rev. D **48**, 2313 (1993)
20. T. Hatsuda, Y. Koike, S.H. Lee, Nucl. Phys. B **394**, 221 (1993)
21. S. Mallik, K. Mukherjee, Phys. Rev. D **58**, 096011 (1998); D **61**, 116007 (2000)
22. S. Mallik, S. Sarkar, Phys. Rev. D **65**, 016002 (2002)
23. For formal proofs, see S. Mallik, Eur. Phys. J. C **24**, 143 (2002)
24. V.L. Eletsky, M. Belkacem, P.J. Ellis, J.I. Kapusta, nucl-th/0104029
25. A.J. Niemi, G.W. Semenoff, Ann. Phys. (N.Y.) **152**, 105 (1984)
26. R.L. Kobes, G.W. Semenoff, Nucl. Phys. B **260**, 714 (1985)